Electric Power Systems Research 97 (2013) 144–150

Contents lists available at SciVerse ScienceDirect

Electric Power Systems Research

journal homepage: www.elsevier.com/locate/epsr

Maximum power extraction from wind energy system based on fuzzy logic control

Ali M. Eltamaly, Hassan M. Farh*

Sustainable Energy Technologies Center, Department of Electrical Engineering, College of Engineering, King Saud University, P.O. Box 800, Riyadh 11421, Saudi Arabia

ARTICLE INFO

Article history:
Received 7 October 2012
Received in revised form
11 December 2012
Accepted 7 January 2013
Available online 30 January 2013

Keywords:
Wind energy systems
Permanent magnet synchronous generator
Fuzzy logic controller
Simulation software packages (PSIM and Simulink)
Maximum power point tracking

ABSTRACT

This paper proposes a variable speed control scheme for grid-connected wind energy conversion system (WECS) using permanent magnet synchronous generator (PMSG). The control algorithm tracks the maximum power for wind speeds below rated speed of wind turbines and ensures the power will not go over the rated power for wind speeds over the rated value. The control algorithm employs fuzzy logic controller (FLC) to effectively do this target. The wind turbine is connected to the grid via back-to-back PWM-VSC. Two effective computer simulation packages (PSIM and Simulink) are used to carry out the simulation effectively. The control system has two controllers for generator side and grid side converters. The main function of the generator side controller is to track the maximum power through controlling the rotational speed of the wind turbine using FLC. In the grid side converter, active and reactive power control has been achieved by controlling *q*-axis and *d*-axis current components, respectively. The *d*-axis current is set at zero for unity power factor and the *q*-axis current is controlled to deliver the power flowing from the dc-link to the electric utility grid.

1. Introduction

Wind energy is one of the most promising renewable energy resources for generating electricity due to its cost competitiveness compared to other conventional types of energy resources. Only some specific locations with adequate wind energy resources can be described as being suitable for wind energy electricity generation. Wind energy is not harmful to the environment and it is naturally an abundant resource. Hence, wind power could be utilized by mechanically converting it to electrical power using wind turbine (WT). Various WT concepts have been developed into wind power technologies and led to significant growth of wind power capacity during the last two decades. Variable speed operation and direct drive WTs have been the modern aspects of the wind energy conversion system (WECS) technology. Variable-speed has many advantages over fixed-speed operations such as increased energy capture, operation at maximum power point over a wide range of wind speeds, high power quality, reduced mechanical stresses, aerodynamic noise improved system reliability, providing 10–15% higher output power and less mechanical stresses compared to the operation of a fixed speed systems [1,2]. WTs can be classified into direct drive (DD) and geared drive (GD) according to the type of drive train. The GD type uses a gear box and squirrel cage induction generator (SCIG). The GD configuration can be classified into stall, active stall and pitch control systems in constant speed applications. The variable speed applications used doubly-fed induction generator (DFIG) especially in high power WTs. The gearless DD WTs have been used with small and medium size WTs employing PMSG with higher numbers of poles to eliminate the need for gearbox which can be translated into higher efficiency. PMSG appears more and more attractive, because of the advantages of permanent magnet (PM) machines over electrically excited machines such as its higher efficiency, higher energy per weight, and no additional power supply for the magnet field excitation and higher reliability due to the absence of mechanical components such as slip rings. In addition, the performance of PM materials is improving and the cost is decreasing in recent years. Therefore, these advantages make DD applications in PM wind turbine generator systems more attractive in application of small and medium-scale wind turbines [1,3,4].

Robust controller has been developed in many literatures [5–15] to track the maximum power available in the wind. They include tip speed ratio (TSR) [5,13], power signal feedback (PSF) [8,14] and the hill-climb searching (HCS) [11,12] techniques. The TSR control technique regulates the rotational speed of the generator to maintain an optimal TSR at which maximum power is extracted [13]. For TSR calculation, both the wind speed and turbine speed need to be measured, and the optimal TSR must be given to the controller. The first barrier to implement TSR control technique is the wind speed measurement which adds to system cost and presents difficulties in practical implementations. The second barrier is the need to obtain the optimal value of TSR; this value is different from one system

* Corresponding author. Tel.: +966 500507630.
E-mail address: hfarh1@ksu.edu.sa (H.M. Farh).

0378-7796/$ – see front matter © 2013 Elsevier B.V. All rights reserved.
http://dx.doi.org/10.1016/j.epsr.2013.01.001

to another. This depends on the turbine-generator characteristics results in custom-designed control software tailored for individual wind turbines [14]. In PSF control technique [8,14], it is required to have the knowledge of the wind turbine's maximum power curves to track its maximum power point in these curves through its control mechanisms. The power curves need to be obtained via simulations or off-line experiment on individual wind turbines or from the datasheet of WT which makes it difficult to implement with accuracy in practical applications [7,8,15]. The HCS technique does not require wind speed data, generator rotational speeds measurements or the turbine characteristics. But, this technique works well only for very small wind turbine inertia. For large inertia wind turbines, the system output power is interlaced with the turbine mechanical power and rate of change in the mechanically stored energy, which often renders the HCS technique ineffective [11,12]. On the other hand, different algorithms have been used for maximum power extraction from WT in addition to the three techniques mentioned above. For example, Oghafy [1] presents an algorithm for maximum power extraction and reactive power control of an inverter through the power angle (δ) of the inverter terminal voltage and the modulation index (m_a) based on variable-speed WT without wind speed sensor. Chinchilla et al. [16] present an algorithm for maximum power point tracking (MPPT) via controlling the generator torque through q-axis current and hence controlling the generator speed with variation of the wind speed. These techniques are used for a decoupled control of the active and reactive power generated from the WT through q-axis and d-axis current respectively. Also, Song et al. [17] present a decoupled control of the active and reactive power generated from the WT, independently through q-axis and d-axis current but maximum power point operation of the WECS has been produced through regulating the input dc current of the dc/dc boost converter to follow the optimized current reference. Eltamaly [18] presents an algorithm for MPPT through directly adjusting duty ratio of the dc/dc boost converter and modulation index of the PWM-VSC. Hussein et al. [19] present MPPT control algorithm based on measuring the dc-link voltage and current of the uncontrolled rectifier to attain the maximum available power from wind. Finally, MPPT control based on a fuzzy logic control (FLC) has been presented in [20–22]. The function of FLC is to track the generator rotational speed with the reference speed for maximum power extraction with variation of wind speeds.

In this study, the WECS is designed using PMSG connected with the grid via a back-to-back PWM-VSC as shown in Fig. 1. A modified MPPT control algorithm has been introduced using FLC to regulate the rotational speed to force the PMSG to work around its maximum power point in speeds below rated speeds and to produce the rated power in wind speed higher than the rated wind speed of the WT. The input to FLC is two real time measurements which are the change of output power and rotational speed between two consequent iterations (ΔP_m, and $\Delta\omega_m$). The output from FLC is the required change in the rotational speed $\Delta\omega_m^*$. The detailed logic behind the new proposed technique is explained in details in the following sections. Indirect vector-controlled PMSG system has been used for this purpose. The modified MPPT control system shown in this paper is able to track maximum output power via controlling the electromagnetic torque using the two components i_α, i_β of the generator current in simple and effective way. For the grid side converter, active and reactive power control has been achieved by controlling quadrature and direct current components of grid current respectively. Two effective computer simulation software packages (PSIM and Simulink) have been integrated together to carry out the simulation of the modified system effectively. PSIM contains the power circuit of the WECS and Matlab/Simulink contains the control circuit of the WECS. The idea behind integrating these two different software packages is that PSIM is a very effective and a simple tool for modeling the power electronics circuits whereas Simulink is a very effective and a simple tool for modeling the control system especially for FLC and mathematical manipulation. This integration between PSIM and Simulink has never been used in MPPT of wind energy systems in the literature and this approach will help researchers to develop many other control techniques in this area. The interconnection between PSIM and Simulink makes the simulation process easier, efficient, fast response and powerful.

2. Wind energy conversion system description

Fig. 2 shows the co-simulation (PSIM/Simulink) programs for interconnecting WECS to electric utility. The PSIM program contains the power circuit of the WECS and Matlab/Simulink program contains the control of this system. The connection between PSIM and Matlab/Simulink has been done via the SimCoupler block tool in Simulink. The basic topology of the power circuit which has PMSG driven wind turbine connected to the utility grid through the ac–dc–ac conversion system is shown in Fig. 1. The PMSG is connected to the grid via back-to-back bidirectional PWM-VSC. The generator side converter is connected to the grid side converter through dc-link capacitor. The control of the overall system has been done through the generator side converter and the grid side converter. The MPPT algorithm has been achieved through controlling the generator side converter using FLC. The grid-side converter controller maintains the dc-link voltage at the desired value by exporting active power to the grid and it controls the reactive power exchange with the grid.

2.1. Wind turbine model

Wind turbine converts the wind power to a mechanical power. This mechanical power generated by wind turbine at the shaft of the generator can be expressed as:

$$P_m = \frac{1}{2} C_P(\lambda, \beta)\rho A u^3 \quad (1)$$

where ρ is the air density (typically 1.225 kg/m^3), β is the pitch angle (in degree), A is the area swept by the rotor blades (in m^2), u

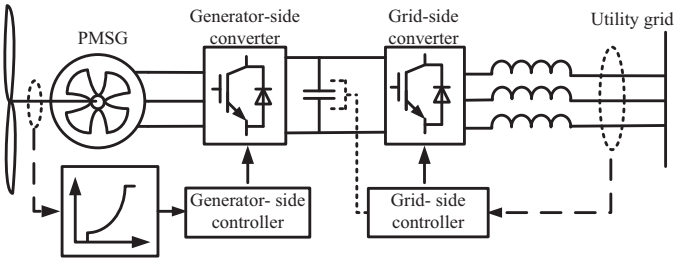

Fig. 1. Schematic diagram of the overall system.

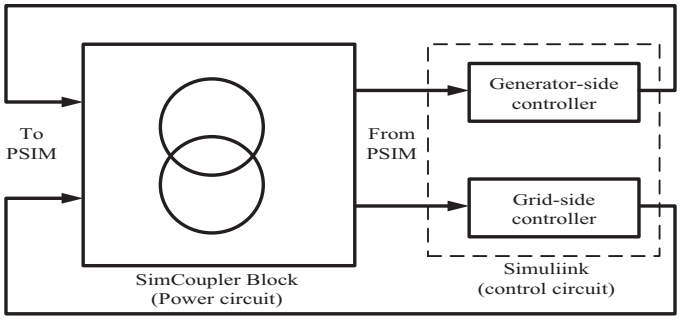

Fig. 2. Co-simulation block of wind energy system interfaced to electric utility.

is the wind speed (in m/s) and $C_P(\lambda, \beta)$ is the wind-turbine power coefficient (dimensionless).

The turbine power coefficient, $C_P(\lambda, \beta)$, describes the power extraction efficiency of the wind turbine. It is defined as the ratio between the mechanical power available at the turbine shaft and the power available in wind. A generic equation is used to model $C_P(\lambda, \beta)$ based on the modeling turbine characteristics and it is shown as follows [23]:

$$C_P(\lambda, \beta) = 0.5176\left(116 * \frac{1}{\lambda_i} - 0.4\beta - 5\right) e^{-21/\lambda_i} + 0.0068\lambda \quad (2)$$

where $1/\lambda_i = 1/(\lambda + 0.08\beta) - (0.035/1 + \beta^3)$.

C_P is a nonlinear function of both tip speed ratio (λ) and the blade pitch angle (β). λ is the ratio of the turbine speed ($\omega_m^* R$) to the wind speed (u) as follow [24]:

$$\lambda = \frac{\omega_m^* R}{u} \quad (3)$$

where ω_m is the rotational speed and R is the radius of the swept area by turbine blades, respectively.

For a fixed β, C_P becomes a nonlinear function of λ, only. According to Eq. (3), there is a relation between λ and ω_m. Hence, at a certain u, the power is maximized at a certain ω_m called optimum rotational speed, ω_{opt}. This speed corresponds to optimum tip speed ratio (λ_{opt}) [15]. The value of the tip speed ratio is constant for all maximum power points (MPPs). So, to extract maximum power at variable wind speed, the WT should always operate at λ_{opt} in speeds bellow the rated speed. This occurs by controlling the rotational speed of the WT to be equal to the optimum rotational speed. Fig. 3 shows that the mechanical power generated by WT at the shaft of the generator as a function of ω_m. These curves are obtained from PSIM technical support team for the wind turbine used in this paper. It is clear from this figure that for each wind speed; the mechanical output power is maximized at particular rotational speed (ω_{opt}).

2.2. PMSG model

The generator is modeled by the following voltage equations in the rotor reference frame (dq axes) [25]:

$$v_{sd} = R_s i_{sd} + \frac{d\lambda_{sd}}{dt} - \omega_r \lambda_{sq}$$
$$v_{sq} = R_s i_{sq} + \frac{d\lambda_{sq}}{dt} + \omega_r \lambda_{sd} \quad (4)$$

where λ_{sq}, and λ_{sd} are the stator flux linkages in the direct and quadrature axis of rotor. The equations for these values in the absence of damper circuits can be expressed in terms of the stator currents and the magnetic flux as following [25]:

$$\lambda_{sd} = L_s i_{sd} + \psi_F$$
$$\lambda_{sq} = L_s i_{sq} \quad (5)$$

where ψ_F is the flux of the permanent magnets, L_s is the stator inductance of PMSG.

The electrical torque, T_e of the three-phase PMSG can be calculated as following [25,26]:

$$T_e = \frac{3}{2} P[\lambda_{sd} i_{sq} - \lambda_{sq} i_{sd}] \quad (6)$$

where P is the number of pole pairs. For a non-salient-pole machine, the stator inductances L_{sd} and L_{sq} are approximately equal [25]. This means that the direct-axis current i_{sd} does not contribute to the electrical torque. Our concept is to keep i_{sd} to zero in order to obtain maximal torque with minimum current. Then, the electromagnetic torque can be obtained from the following equation:

$$T_e = \frac{3}{2} P \psi_F i_{sq} = K_c i_{sq} \quad (7)$$

where i_{sq} is the quadrature-axis component of the stator-current space vector expressed in the rotor reference frame and K_c is called the torque constant.

3. Control of the generator side converter

The generator side controller controls the generator rotational speed to produce the maximum output power via controlling the electromagnetic torque according to Eq. (7). The proposed control logic of the generator side converter is shown in Fig. 4. The speed loop will generate the q-axis current component to control the generator torque and speed at different wind speed via estimating the references value of i_α, i_β as shown in Fig. 4. The torque control can be achieved through the control of the i_{sq} current as shown in Eq. (7). Fig. 5 shows the stator and rotor current space phasors and the excitation flux of the PMSG. The quadrature stator current i_{sq} can be controlled through the rotor reference frame (α, β axis) as shown in Fig. 5 [25]. So, the references value of i_α, i_β can be estimated easily from the amplitude of i_{sq}^* and the rotor angle, θ_r. Initially, to find the rotor angle, θ_r, the relationship between the electrical

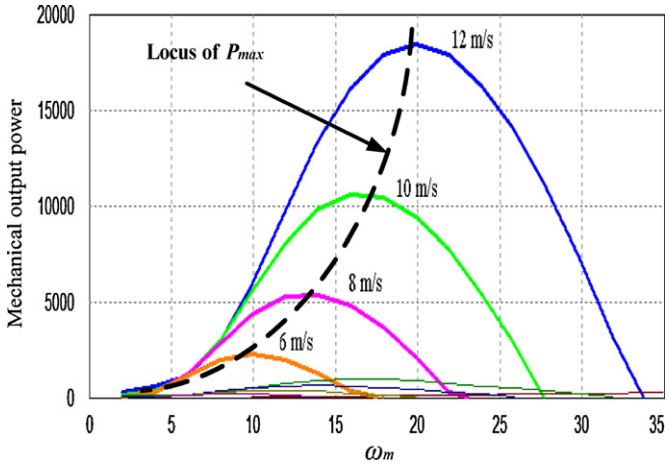

Fig. 3. Typical output power characteristics.

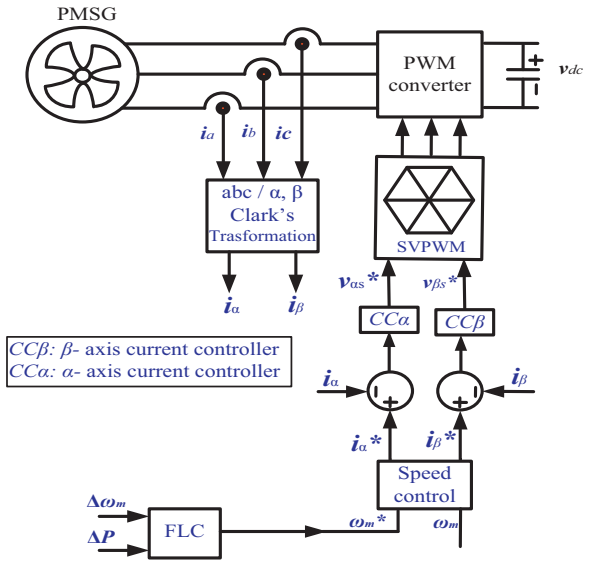

Fig. 4. Control block diagram of generator side converter.

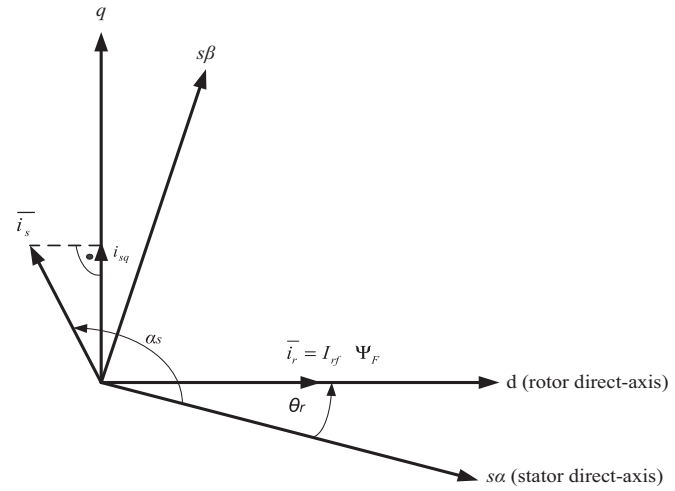

Fig. 5. The stator and rotor current space phasors and the excitation flux of the PMSG.

angular speed, ω_r and the rotor mechanical speed (rad/s), ω_m can be expressed as:

$$\omega_r = \frac{P}{2}\omega_m \tag{8}$$

So, the rotor angle, θ_r can be estimated by integrating of the electrical angular speed, ω_r. The input to the speed control is the actual and reference rotor mechanical speed (rad/s) and the output is the (α, β) reference current components. The actual values of the (α, β) current components have been estimated using Clark's transformation to the three phase current of PMSG. The FLC can be used to find the reference speed along which tracks the MPPs.

4. Fuzzy logic controller for MPPT

At certain wind speed, the power is maximized at a certain ω_m called optimum rotational speed (ω_{opt}). This speed corresponds to optimum tip speed ratio (λ_{opt}) [15]. So, to extract maximum power at variable wind speed, the turbine should always operate at λ_{opt}. This occurs by controlling the rotational speed of the turbine. Controlling of the turbine to operate at optimum rotational speed can be done using the FLC. Each wind turbine has one value of λ_{opt} at variable speed but ω_{opt} changes from a certain wind speed to another. From Eq. (3), the relation between ω_{opt} and wind speed (u) for constant R and λ_{opt} can be obtained as following:

$$\omega_{opt} = \frac{\lambda_{opt}}{R}u \tag{9}$$

From Eq. (9), the relation between the optimum rotational speed and wind speed is linear. FLC is used to search the rotational speed reference which tracks the maximum power point at variable wind speeds. The block diagram of FLC is shown in Fig. 6. The main goal of implementing FLC instead of using PI-controller is to

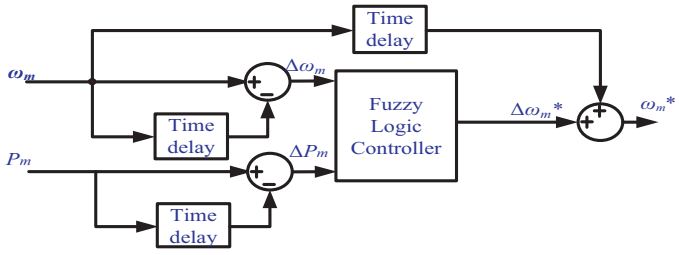

Fig. 6. Input and output of fuzzy controller.

Table 1
Rules of fuzzy logic controller.

$\Delta\omega_m$	ΔP_m								
	N++	NB	NM	NS	ZE	PS	PM	PB	P++
N	P++	PB	PM	PS	ZE	NS	NM	NB	N++
ZE	NB	NM	NS	NS	ZE	PS	PM	PM	PB
P	N++	NB	NM	NS	ZE	PM	PM	PB	PB

continuously adapt the rotational speed of the generator to the wind speed in a way that the turbine operates at its optimum level of aerodynamic efficiency. The advantages of using FLC against standard PI-controller are universal control algorithm, very simple, adaptive, fast response, extension of the operating range, parameter insensitivity and it can work properly even with an inaccurate input signals. The proposed FLC doesn't need any information on the wind speed or WT parameters which makes it universal for different WT types. Also, FLC has better and efficient response in tracking the maximum power point, especially in case of frequently changing wind speeds. Two variables are used as input to FLC (ΔP_m, and $\Delta\omega_m$) and the output is ($\Delta\omega_m^*$). Membership functions are shown in Fig. 7. Triangular symmetrical membership functions are suitable for the input and output, which give more sensitivity especially as variables approach to zero value. FLC does not require any detailed mathematical model of the system and its operation is governed simply by a set of rules. The principle of the FLC is to perturb the reference speed, $\Delta\omega_m^*$ and to observe the corresponding change of power, ΔP_m. If the output power increases with the last speed increment, the searching process continues in the same direction. On the other hand, if the speed increment reduces the output power, the direction of the searching is reversed. The FLC is efficient to track the maximum power point, especially in case of frequently changing wind conditions [22].

Fig. 7 shows the input and output membership functions. Table 1 lists the control rule for the input and output variable. The next fuzzy levels are chosen for controlling the inputs and output of the FLC. The variation step of the power and the reference speed may vary depending on the system. In Fig. 7, the variation step in the speed reference is from −0.15 rad/s to 0.15 rad/s for power variation ranging over from −30 W to 30 W. The membership definitions are given as follows: N (negative), N++ (very big negative), NB (negative big), NM (negative medium), NS (negative small), ZE (zero), P (positive), PS (positive small), PM (positive medium), PB (positive big), and P++ (very big positive).

5. Control of the grid side converter

The power flow of the grid-side converter is controlled in order to maintain the dc-link voltage at reference value, 600 V. Since increasing the output power rather than the input power to

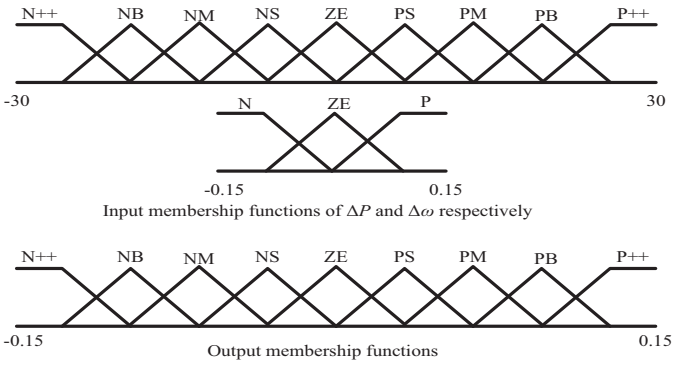

Fig. 7. Membership functions of fuzzy logic controller.

dc-link capacitor causes a decrease of the dc-link voltage and vice versa. The output power will be regulated to keep dc-link voltage approximately constant. The dc-link voltage has been maintained and the reactive power flowing into the grid has been controlled at zero value. This has been done via controlling the grid side converter currents using the d–q vector control approach. The active and reactive power can be defined as the following:

$$P_s = \frac{3}{2}(v_d i_d + v_q i_q) \tag{10}$$

$$Q_s = \frac{3}{2}(v_q i_d - v_d i_q) \tag{11}$$

By aligning the q-axis of the reference frame along with the grid voltage position $v_d = 0$ and from (10) and (11) the active and reactive power can be obtained from the following equations:

$$P_s = \frac{3}{2} v_q i_q \tag{12}$$

$$Q_s = \frac{3}{2} v_q i_d \tag{13}$$

Active and reactive power control has been achieved by controlling quadrature and direct grid current components respectively. Two control loops are used to control the active and reactive power. An outer dc-link voltage control loop is used to set the q-axis current reference for active power control. The inner control loop controls the reactive power by setting the d-axis current reference to zero value for unity power factor as shown in Eq. (13). The q-axis current is controlled to deliver the power flowing from the dc-link to the grid to maintain the dc-link voltage at constant value. The control block diagram of the grid side converter is shown in Fig. 8.

6. Simulation results

A co-simulation (PSIM/Simulink) program has been used where PSIM contains the power circuit of the WECS and Matlab/Simulink has the whole control system as described before. The model of WECS in PSIM contains the WT connected to the utility grid through back-to-back bidirectional PWM converter. The control of the whole system in Simulink contains the generator side controller and the grid side controller. The wind turbine characteristics and the parameters of the PMSG are listed in the Appendix. The generator can be directly controlled by the generator side controller to track the maximum power available from the WT. The wind speed has been taken from actual wind speed data from Dammam site in Saudi Arabia where these wind speeds is changing from 7 m/s to 13 m/s as input to WT as shown in Fig. 9(a). To extract maximum power at variable wind speed, the turbine should always operate at λ_{opt}. This occurs by controlling the rotational speed of

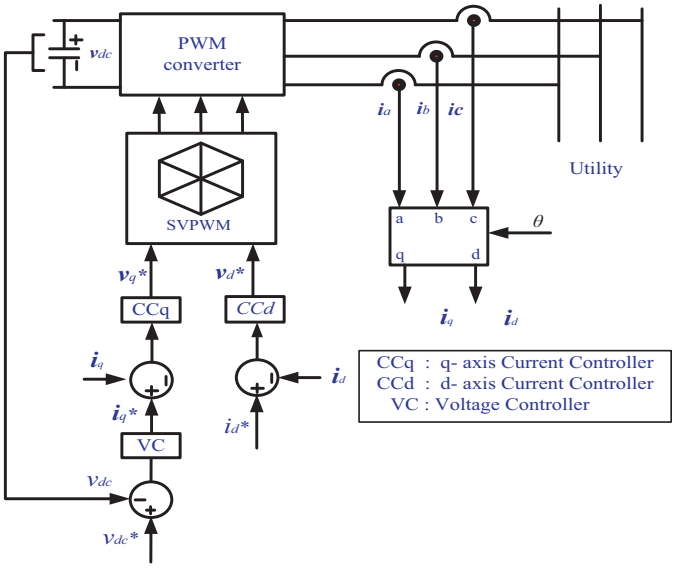

Fig. 8. Control block diagram of grid-side converter.

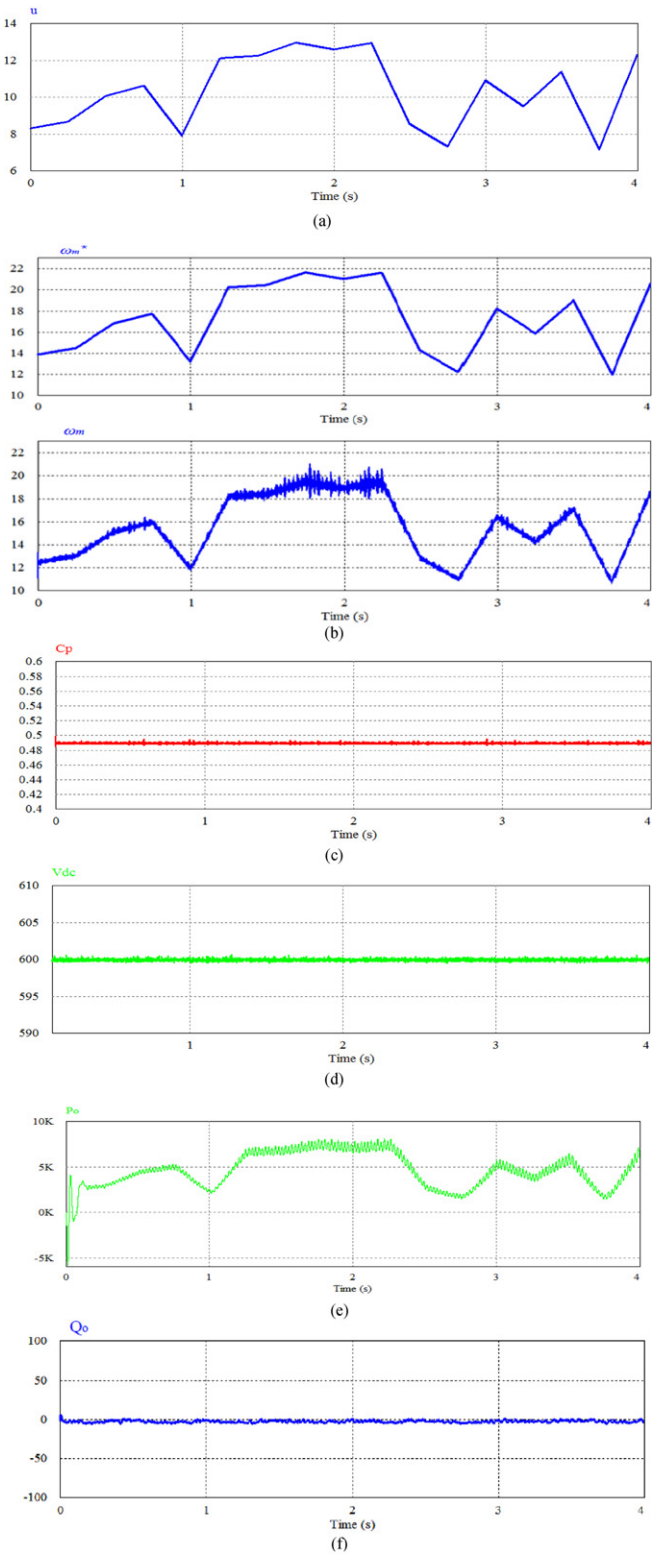

Fig. 9. Different simulation waveforms: (a) wind speed variation (7–13) m/s, (b) actual and reference rotational speed (rad/s), (c) C_P, (d) dc-link voltage (v), (e) active power (W), and (f) reactive power (Var).

the WT. So, it always operates at ω_{opt}. Where, ω_{opt} changes from a certain wind speed to another. The fuzzy logic controller is used to search the optimum rotational speed which tracks the maximum power point at variable wind speeds. On the other hand, Fig. 9(b) shows the variation of the actual and reference rotational speed as a result of the wind speed variation. At certain wind speed, the actual and reference rotational speeds are estimated and these values agree with the power characteristic of the wind turbine shown previously in Fig. 3. Hence the WT always operates at the optimum rotational speed which proves the superiority of the proposed FLC in accurately tracking performance for the maximum output power point and forcing the WT to rotate at the optimum rotational speed. Hence, the power extraction from wind is maximized at variable wind speed. It is clear from Fig. 9(b) that the control system follows the reference speed which obtained from FLC. Fig. 9(c) shows the power coefficient (C_P) waveform. The grid-side controller maintains the dc-link voltage at the desired value, 600 V, as shown in Fig. 9(d). The dc-link voltage is regulated by exporting active power to the grid as shown in Fig. 9(e). The reactive power transmitted to the grid has been controlled to be zero as shown in Fig. 9(f). The results obtained from Fig. 9 show that the control system is working effectively in tracking the maximum power and accurately control the reactive power as required from the grid.

7. Conclusions

A co-simulation (PSIM/Simulink) program has been proposed for WECS in this paper where PSIM contains the power circuits of the WECS and Matlab/Simulink contains the control circuit of the WECS. The idea behind integrating these two software packages is that, the Matlab/Simulink is a powerful tool for modeling the control system, FLC and mathematical manipulation whereas PSIM is a powerful tool for modeling power electronics circuits and switches. Co-simulation (PSIM/Simulink) makes the simulation process so much easy, efficient, faster in response and powerful. The integration between PSIM and Simulink is the first time to be used in modeling WECS which help researchers in modifying the modeling of WECS in the future. The WT is connected to the grid via back-to-back PWM converters which have been modeled in PSIM. The generator side and the grid side controllers have been modeled in Simulink. The generator side controller has been used to track the maximum power generated from WT through controlling the rotational speed of the turbine using FLC. The PMSG has been controlled in indirect-vector field oriented control technique and its speed reference has been obtained from FLC. In the grid side converter, active and reactive power control has been achieved by controlling q-axis and d-axis grid current components respectively. The d-axis grid current is controlled to be zero for unity power factor and the q-axis grid current is controlled to deliver the power flowing from the dc-link to the grid. The simulation results prove the superiority of FLC and the whole control system.

Acknowledgments

The authors acknowledge the National Plan for sciences and Technology program's Project No. ENE226-02-08 by King Saud University for the financial support to carry out the research work reported in this paper.

Appendix.

List of symbols

δ	the power angle of PWM converter
m_a	the modulation index of the PWM-VSC
D	duty ratio of the boost converter
C_P	the wind-turbine power coefficient
u	the wind speed (m/s)
λ, β	the tip speed ratio and the pitch angle of wind turbine blades
λ_{sq}	the stator flux linkages in the q-axis of rotor
λ_{sd}	the stator flux linkages in the d-axis of rotor
ψ_F	the flux of the permanent magnets
i_{sq}	the quadrature-axis component of the stator-current
i_{sd}	the direct-axis component of the stator-current
T_e	the electromagnetic torque
θ_r	the rotor angle
ω_r	the electrical angular speed
ω_m	the rotor mechanical speed
P_m	output power from WT generator
P_s, Q_s	output active and reactive power from the PWM converter to grid respectively

Table A1 Parameters of wind turbine model and PMSG.

Wind turbine		PMSG	
Nominal output power	19 kw	R_s (stator resistance)	1 m
Wind speed input	7:13 m/s	L_d (d-axis inductance)	1 m
Base wind speed	12 m/s	L_q (q-axis inductance)	1 m
Base rotational speed	190 rpm	No. of poles, P	30
Moment of inertia	1 m	Moment of inertia	100 m
Blade pitch angle input	0°	Mech. time constant	1

References

[1] V. Oghafy, H. Nikkhajoei, Maximum power extraction for a wind-turbine generator with no wind speed sensor, in: Proceedings on IEEE, Conversion and Delivery of Electrical Energy in the 21st Century, 2008, pp. 1–6.
[2] T. Ackerman, L. Söder, An overview of wind energy status 2002, Renewable and Sustainable Energy Reviews 6 (2002) 67–128.
[3] M.R. Dubois, Optimized permanent magnet generator topologies for direct-drive wind turbines, Ph.D. dissertation, Delft Univ. Technol., Delft, The Netherlands, 2004.
[4] A. Grauers, Design of direct-driven permanent-magnet generators for wind turbines, Ph.D. dissertation, Chalmers Univ. Technol., Goteborg, Sweden, 1996.
[5] T. Thiringer, J. Linders, Control by variable rotor speed of a fixed pitch wind turbine operating in a wide speed range, IEEE Transactions on Energy Conversion EC-8 (1993) 520–526.
[6] I.K. Buehring, L.L. Freris, Control policies for wind energy conversion system, Proceeding of the Institute of Electrical and Electronic Engineers C 128 (1981) 253–261.
[7] M. Erimis, H.B. Ertan, E. Akpinar, F. Ulgut, Autonomous wind energy conversion systems with a simple controller for maximum power transfer, Proceeding of the Institute of Electrical and Electronic Engineers B 139 (1992) 421–428.
[8] R. Chedid, F. Mrad, M. Basma, Intelligent control of a class of wind energy conversion systems, IEEE Transactions on Energy Conversion EC-14 (1999) 1597–1604.
[9] M.G. Simoes, B.K. Bose, R.J. Spiegal, Fuzzy logic-based intelligent control of a variable speed cage machine wind generation system, IEEE Transactions on Power Electronics PE-12 (1997) 87–94.
[10] J.H. Enslin, J.V. Wyk, A study of a wind power converter with micro-computer based maximum power control utilizing an over-synchronous electronic Scherbius cascade, Renewable Energy World 2 (6) (1993) 551–562.
[11] Q. Wang, L. Chang, An intelligent maximum power extraction algorithm for inverter-based variable speed wind turbine systems, IEEE Transactions on Power Electronics 19 (5) (2004) 1242–1249.
[12] Q. Wang, Maximum wind energy extraction strategies using power electronic converters, Ph.D. dissertation, University of New Brunswick, Canada, 2003.
[13] H. Li, K.L. Shi, P.G. McLaren, Neural-network-based sensorless maximum wind energy capture with compensated power coefficient, IEEE Transactions on Industry Applications 41 (6) (2005) 1548–1556.
[14] A.B. Raju, B.G. Fernandes, K. Chatterjee, A UPF power conditioner with maximum power point tracker for grid connected variable speed wind energy conversion system, in: Proceedings of the First International Conference on PESA, Bombay, India, 2004, pp. 107–112.
[15] M.A. Abdullah, A.H.M. Yatim, C. Wei Tan, A study of maximum power point tracking algorithms for wind energy system, in: Proceedings of the First IEEE Conference on Clean Energy and Technology CET, 2011, pp. 321–326.
[16] M. Chinchilla, S. Arnaltes, J.C. Burgos, Control of permanent-magnet generators applied to variable-speed wind-energy systems connected to the grid, IEEE Transactions on Energy Conversion 21 (March (1)) (2006) 130–135.

[17] S. Song, S. Kang, N. Hahm, Implementation and control of grid connected AC–DC–AC power converter for variable speed wind energy conversion system, IEEE (2003) 154–158.
[18] A.M. Eltamaly, Modelling of wind turbine driving permanent Magnet Generator with maximum power point tracking system, Journal of King Saud University 19 (2) (2007) 223–237.
[19] M.M. Hussein, M. Orabi, M.E. Ahmed, M.A. Sayed, Simple sensorless control technique of permanent magnet synchronous generator wind turbine, in: Proceedings of the IEEE International Conference on Power and Energy, PEC2010, Kuala Lumpur, Malaysia, 2010, pp. 512–517.
[20] S. Pati, K.B. Mohanty, B. Sahu, Performance comparison of a robust self tuned fuzzy logic controller used for power control in wind conversion systems, in: Proceedings of Modern Electric Power Systems, MEPS'10, Wroclaw, Poland, September, 2010, pp. 20–22.
[21] X. Yao, C. Guo, Z. Xing, Y. Li, S. Liu, Variable speed wind turbine maximum power extraction based on fuzzy logic control, in: Proceedings of International Conference on Intelligent Human–Machine Systems and Cybernetics, IEEE, 2009, pp. 202–205.
[22] A.G. Abo-Khalil, D.C. Lee, J.K. Seok, Variable speed wind power generation system based on fuzzy logic control for maximum power output tracking, in: Proceedings of the 35th Annual IEEE Power Electronics Specialists Conference, PESC, Aachen, Germany, 3, 2004, pp. 2039–2043.
[23] S. Heier, Grid Integration of Wind Energy Conversion Systems, John Wiley & Sons, Germany, 2006.
[24] G.L. Johnson, Wind Energy Systems, Prentice Hall, Englewood cliffs, 2003.
[25] P. Vas, Sensorless Vector and Direct Torque Control, Oxford Science Publications, New York, 1998.
[26] N.A. Orlando, M. Liserre, V.G. Monopoli, A. Dell'Aquila, Speed sensorless control of a PMSG for small wind turbine systems, in: Proceedings of IEEE International Symposium on Industrial Electronics, ISIE, Seoul, Korea, July 5–8, 2009, pp. 1540–1545.